Instability of sonoluminescing bubbles under a nonspherical symmetrical acoustic-pressure perturbation

Yu An, Tao Lu, and Bing Yang
Department of Physics, Tsinghua University, Beijing 100084, China
(Received 23 September 2004; published 28 February 2005)

The perturbation of nonspherical symmetrical acoustic pressure is added to the equation governing the spherical stability of sonoluminescing bubbles. The numerical calculations of the shape instability of sonoluminescing bubbles with the modified equation are conducted and the results are illustrated accordingly in the p_a-R_0 phase diagrams. The calculated results indicate that the stability region vanishes as the amplitude of the driving acoustic pressure p_a arrives at the upper threshold ($\sim$1.6 atm) due to the perturbation of a small nonspherical symmetrical acoustic pressure (about a few Pa), which is in consistence with the experimental observations.

DOI: 10.1103/PhysRevE.71.026310 PACS number(s): 78.60.Mq, 47.20.Gv

INTRODUCTION

A single oscillating gas bubble can be trapped at the velocity node of an acoustic standing wave in water. The bubble usually oscillates hundreds of million times uninterruptedly in harmony with the oscillation of the acoustic field and emits synchronous picoseconds light pulses, which is known as the single-bubble sonoluminescence (SBSL) [1,2]. Experiments show that the stable SBSL is restricted in a narrow parameter area, which is the result of the instabilities of shape [3,4], diffusion [5], and chemical reactions [6]. With the consideration of the driving frequency in the range of 20–30 kHz, it has been revealed by experiments conducted a few years ago that the stable SBSL region has the upper threshold of the ambient radius R_0 and of the amplitude of the driving acoustic pressure p_a [7]. The threshold of R_0 is predictable in accordance with the analysis of the shape instability [4], but the prediction of the threshold of p_a itself is not easy. Usually, the threshold of p_a is constrainedly obtained by the dint of thermal noises [4,8], or by computing the amplification factor of an initial distortion (it may be due to the thermal noise) of microscopic sizes only in the primary collapse [9,10] duration. In the present paper, we are concerned with the attention on dynamical factors instead of the adsititious thermal noises. Nevertheless, we do not intend to disavow the existence of the thermal noise effects, but merely attempt to study another possible reason, which we maintain is the prime reason that it limits the unbounded increase of p_a. The basic concept of the present model is to introduce a very small deformation (nonspherical) of the driving sound field as a perturbation. We will see that if the amplitude of this nonspherical symmetrical acoustic pressure is approximately a few Pa ($\sim 10^{-5}$ atm), it would not allow p_a to exceed 1.6 atm or so due to Rayleigh-Taylor (RT) instability, which is just the experimentally observed upper threshold.

THE SHAPE INSTABILITY EQUATION

The shape instability arises out of the deviation from the spherical symmetry of the bubble, and the theory [3] is based on a linear analysis of this deviation. A small distortion of the spherical interface of the bubble is assumed as follows:

$$r = R(t) + a_n Y_n^m(\theta, \phi), \tag{1}$$

where $R(t)$ is the instantaneous bubble mean radius at time t, Y_n^m a surface harmonic function with rank n, and a_n the amplitude of the surface distortion which is independent of the index m in linear region. To determine the radial oscillations of the bubble, we take the uniform approximation in the bubble and consider the effects of water vapor and the heat exchange at the bubble wall, but ignore chemical reactions [11]. The vapor effects are proven to improve the results of the calculation of the shape instability to some extent [12]. The formulas calculating the bubble radius are exactly the same as in Ref. [11] and we shall not repeat them here. Once the mean bubble radius is determined, the distortion a_n can be calculated by the following formulas where a bubble boundary layer type approximation (BLA) is employed [4]:

$$\ddot{a}_n + B_n \dot{a}_n - A_n a_n = 0, \tag{2}$$

with

$$B_n = 3\frac{\dot{R}}{R} - 2(n+2)\left[(n-1)(n+1) - \frac{n(n+2)}{1+2\delta/R}\right]\frac{\eta}{\rho_l R^2}, \tag{3}$$

$$A_n = \frac{(n-1)}{R}\left[\ddot{R} - (n+1)(n+2)\frac{\sigma}{\rho_l R^2} - 2(n+2)\left(n+1 - \frac{n}{1+2\delta/R}\right)\frac{\eta\dot{R}}{\rho_l R^2}\right], \tag{4}$$

where ρ_l, η, and σ are the liquid density, viscosity, and surface tension coefficient, respectively, and δ the boundary layer thickness, simply defined as [4,13]

$$\delta = \min\left(\sqrt{\frac{\eta}{\rho_l \omega}}, \frac{R}{2n}\right), \tag{5}$$

where ω is the frequency of the driving sound field. The full numerical simulation considering viscous nonlocal effects [14] revealed that the results by Eq. (5) underestimated the

threshold of R_0 at $p_a > 1$ atm. For this reason, we simply diminish the estimated value of δ by redefining it in the following formula:

$$\delta = \min\left(k\sqrt{\frac{\eta}{\rho_l \omega}}, \frac{R}{2n}\right), \tag{6}$$

where $0 < k < 1$ for $p_a > 1$ atm, which can raise the threshold of R_0 and improve the accuracy of the BLA to some extent.

The calculation determining parametric instability (PI) by Eqs. (2)–(5) or (6) shows that the initial small distortion ($a_n \sim 10$ nm) may be amplified to infinity or vanished in several or several decades of periods, the dividing line in the p_a-R_0 phase diagrams is just the PI line. Within the calculation, there is no single phase point where a distortion with a finite value can be stably kept on, i.e., the theory of the shape instability on the basis of Eqs. (2)–(5) or (6) does not allow the existence of the stable nonspherical oscillating bubble. However, nonspherical stable sonoluminescing bubbles are experimentally observed [15,16], which requires the improvement in terms of the theory of the shape instability. By reexamining Eq. (2), one can find that the equation is derived under the assumption that the driving sound field is spatially uniform at the location of the bubble where the driving acoustic pressure is $p_s(t) = -p_a \sin(\omega t)$. In accordance with the symmetric analysis, when p_a is not too large, it is apparent that a nonspherical bubble cannot survive for long under the uniform acoustic drive. It is natural, therefore, to introduce a small nonspherical symmetrical acoustic pressure, viz. the distortion of the driving acoustic pressure, and the total driving acoustic pressure is then corrected as the following formula:

$$p_s(t) = -(p_a + \delta p_n Y_n^m)\sin(\omega t). \tag{7}$$

With the correction stated in the formula above, we can rederive Eq. (2) in the same way as in Refs. [3,4]. After neglecting the terms of $1/c_l$, c_l is sound speed in the liquid, we simply have the following formula:

$$\ddot{a}_n + B_n \dot{a}_n - A_n a_n = (n+1)\frac{\delta p_n}{\rho_l R}\sin(\omega t). \tag{8}$$

In the present model, Eqs. (8), (3), and (4), and (5) or (6), are employed to determine the shape instability of the bubbles, where only quadruple distortion, viz., $n=2$, is considered.

It is worthy of mentioning that if one considers the liquid compressibility and retains the first order terms of $1/c_l$ in Eq. (8), the calculated threshold of R_0 at $p_a > 1.3$ atm is much lower than the values measured experimentally, regardless of whether the sound field has a small deformation or not. That is to say, the first order approximation of $1/c_l$ in Eq. (8) is worse than the zeroth.

NUMERICALLY CALCULATED RESULTS

First we consider the experimental data published in Ref. [7]. In the case of Ref. [7], we first calculate the shape instability by neglecting the distortion of the driving acoustic pressure, that is $\delta p_2 = 0$, and compare the results with the different δ defined by Eqs. (5) and (6). Here the k in Eq. (6) is simply chosen as

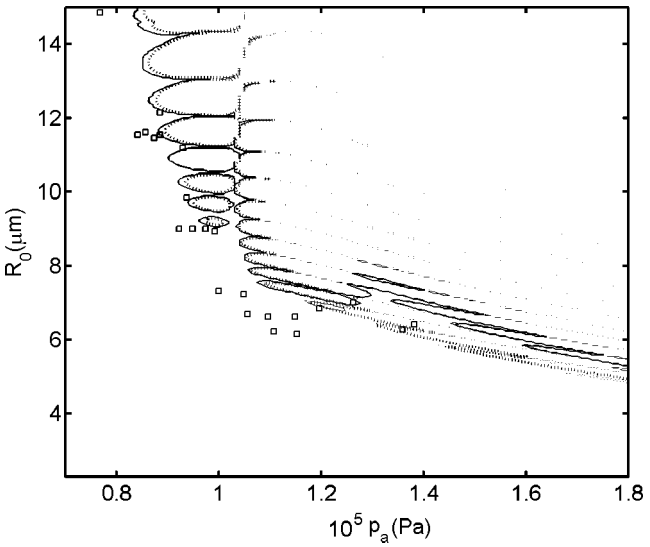

FIG. 1. Calculated PI lines with different δ defined by Eq. (5) (dotted line) and by Eqs. (6) and (9) (solid line), respectively. In both cases, $\delta p_2 = 0$ in Eq. (8), the ambient temperature is 21.7 °C and the frequency of the driving sound field is 20.6 kHz. The experimental data (hollow squares) are digitalized from Ref. [7].

$$k = \begin{cases} 1, & p_a < 1.1 \text{ atm} \\ (1.4 - p_a)/0.3, & 1.1 \text{ atm} \leqslant p_a \leqslant 1.3 \text{ atm} \\ 1/3, & p_a > 1.3 \text{ atm}. \end{cases} \tag{9}$$

Figure 1 shows PI lines with BLA for $n=2$, where one can see the δ defined by Eqs. (6) and (9) makes the instability line higher in the p_a-R_0 phase diagram, which fits with the experimental data much better.

In order to interpret the threshold of p_a, as is argued above, we have to take into account the distortion of the driving acoustic pressure, viz., $\delta p_2 \neq 0$ in Eq. (8) for $n=2$. In the case of $\delta p_2 \neq 0$, the lines of the shape instability are determined by RT instability instead of PI. The criterion of the RT instability used to be expressed as the following formula:

$$\max_{t \subset [0, N(2\pi/\omega)]} \left| \frac{a_n}{R} \right| \geqslant 1, \tag{10}$$

where N is the large number. Figure 2 illustrates the results of $\delta p_2 = 5 \times 10^{-6} p_a$ and $2 \times 10^{-6} p_a$, where we clearly see the threshold of p_a determined by Eq. (10).

Apparently, the larger δp_2 corresponds to the smaller threshold of p_a. This is natural because if the driving sound field at the location of the bubble is less deformed, the larger value of the driving acoustic pressure might be reached at the stable sonoluminescing bubble.

Next we verify the validity of our model through comparing the calculated results to more experimental data available [16–18]. The case shown in Fig. 3 represents an argon bubble driven by the sound field with 32.8 kHz in water at 293 K and an ambient pressure of 1 atm. The experimental data of the critical points of those stable and unstable

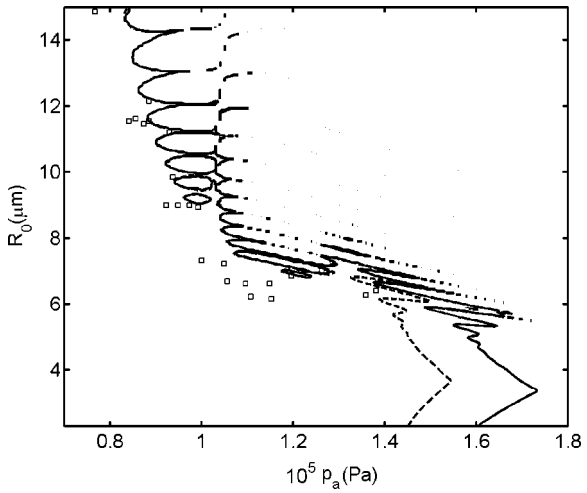

FIG. 2. Calculated RT instability lines with δ defined by Eqs. (6) and (9). $\delta p_2 = 2\times10^{-6}p_a$, $5\times10^{-6}p_a$ correspond to the solid and the dashed lines, respectively. The other parameters are the same as those used in Fig. 1. The experimental data (hollow squares) are digitalized from Ref. [7].

bubbles in p_a-R_0 parametric space are digitalized from Ref. [17]. In the calculation, we take $n=2$, $\delta p_2 = 1.1\times10^{-5}p_a$, and δ defined by Eq. (6) but

$$k=\begin{cases}1, & p_a < 1.0 \text{ atm}\\ 3(3.4/3-p_a)/0.4; & 1.0 \text{ atm} \leqslant p_a \leqslant 1.1 \text{ atm}\\ 1/4, & p_a > 1.1 \text{ atm}.\end{cases} \tag{11}$$

We see the calculated RT instability threshold agrees with the experimental data very well. Figure 4 shows the experimental data from Ref. [18] and the corresponding calculated RT

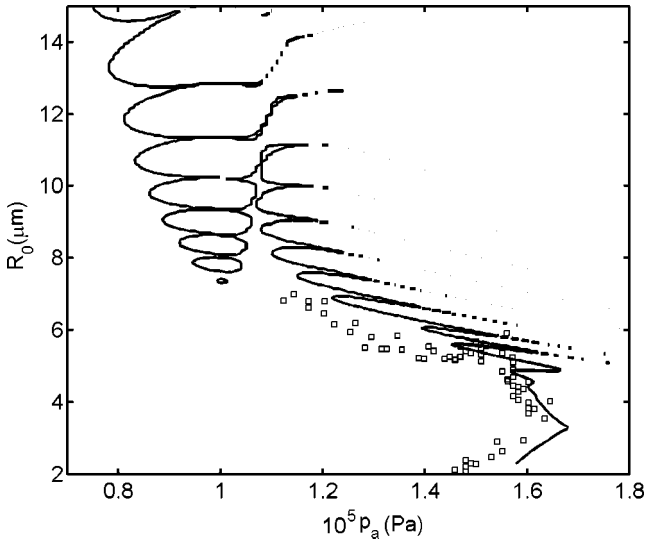

FIG. 3. Calculated RT instability line with δ defined by Eqs. (6) and (11). $\delta p_2 = 1.1\times10^{-5}p_a$, the ambient temperature is 20 °C, and the frequency of the driving sound field is 32.8 kHz. The experimental data of the critical phase points of stable and unstable bubbles (hollow squares) are digitalized from Ref. [17].

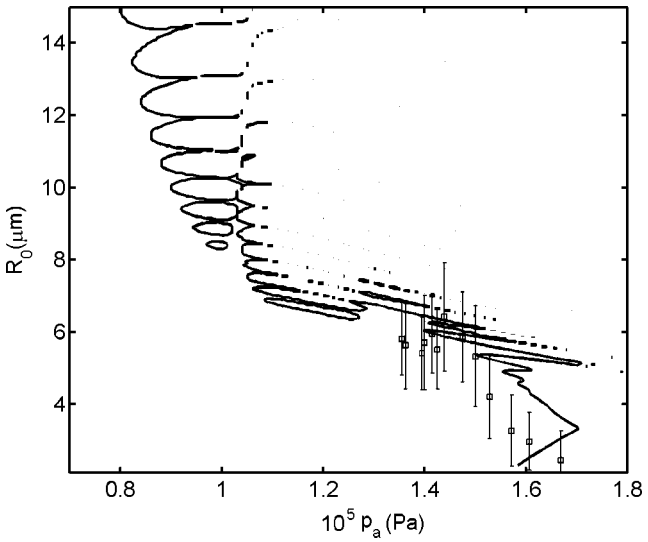

FIG. 4. Calculated RT instability line with δ defined by Eqs. (6) and (9). $\delta p_2 = 3\times10^{-6}p_a$, the ambient temperature is 23.5 °C, and the frequency of the driving sound field is 23.354 kHz. The experimental data (hollow squares with error bar) are digitalized from Ref. [18].

instability threshold with $n=2$, $\boldsymbol{\delta}\mathbf{p}_2 = 3\times10^{-6}\mathbf{p}_a$, and δ defined by Eqs. (6) and (9). We see the calculated threshold of p_a is approximately coincident with the observed data.

Lastly we consider the oscillation of the stable nonspherical bubbles. Some period-doubling phenomena from experimental observation in SBSL are attributed to the stable spherical symmetry breaking of the bubbles [15,16]. In general, for $\delta p_2 \neq 0$, there are regions in the p_a-R_0 phase diagram where the stable nonspherical bubbles are allowed to exist. That is to say, after vibration for a long period, the distortion a_n of a bubble in some regions gradually tends to be a finite value. In Fig. 5, the calculated contour lines with $n=2$, $\delta p_2 = 4\times10^{-6}p_a$, and δ defined by Eq. (5) correspond to $\max_{t\subset[0,N(2\pi/\omega)]}|a_n/R|=1$, the RT instability threshold line, and $\max_{t\to\infty}|a_n/R|=0.5, 0.9$ for $\max_{t\subset[0,N(2\pi/\omega)]}|a_n/R|<1$, respectively. In addition, there are some areas in the phase diagram corresponding to the stable nonspherical bubbles, but they are hard to detect experimentally. The reason is that the maximum value of $|a_n/R|$ during one period appears a few microseconds after the bubble's rebound from its minimum radius. The value of $|a_n/R|$ of the bubble at its minimum radius is very small, see Fig. 6. That is to say, for most of the time in one period, including the time interval of the bubble's flash, the bubble is in a spherical symmetry, even if the maximum value of $|a_n/R|$ is 0.9. The period-doubling phenomenon implies the detectable distortion of the bubble at the moment of the bubble's flashing [16]. The present model is based on a linear analysis of a small distortion; therefore, it cannot cover this phenomenon, which implies that the period-doubling phenomena may contain some nonlinear effects.

CONCLUSION

A small distortion in the driving sound field is introduced to interpret the threshold of the driving acoustic pressure p_a

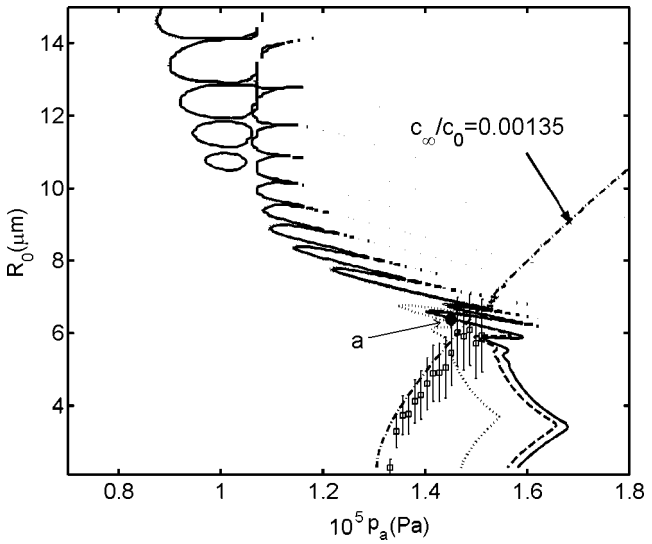

FIG. 5. Calculated curves correspond to $\max_{t\to\infty}|a_n/R|=0.5$ (dotted line), 0.9 (dashed line), and 1.0 (solid line), respectively, with δ defined by Eq. (5), $\delta p_2=4\times10^{-6}p_a$, an ambient temperature of 9 °C, and a frequency of the driving sound field 22.165 kHz. The dashed-dotted line is the calculated diffusive equilibrium curve. The experimental data (hollow squares with error bars) are digitalized from Ref. [16].

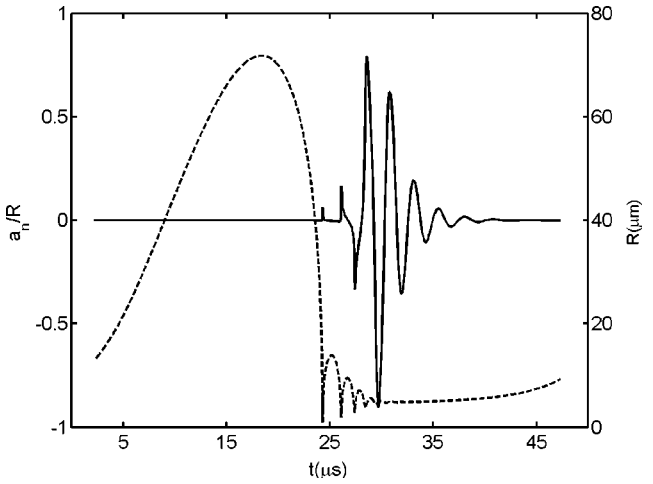

FIG. 6. Calculated bubble radius $R(t)$ (dashed line) and therelative distortion a_n/R (solid line) vs time in the twentieth period of sound field corresponding to point *a* in Fig. 5.

of SBSL. The correction caused by the distortion of the driving acoustic pressure is added to the equation which determines the shape instability of the bubbles. Experimental data from several experiments are well interpreted by the present model and the assumed magnitude of the distortion of the driving acoustic pressure is only about a few Pa. The present model belongs to linear approximation category and thus, it is hard to interpret the period-doubling phenomena.

ACKNOWLEDGMENTS

Y. An is grateful to Professor W. Z. Chen for helpful discussions on the distortion of the driving sound field. This work is supported by NSFC under Grant No. 10174045 and 10434070.

[1] D. F. Gaitan, L. A. Crum, C. C. Church, and R. Roy, J. Acoust. Soc. Am. **91**, 3166 (1992).
[2] B. P. Barber and S. J. Putterman, Nature (London) **352**, 318 (1991).
[3] A. Prosperetti, Q. Appl. Math. **34**, 339 (1977).
[4] S. Hilgenfeldt, D. Lohse, and M. Brenner, Phys. Fluids **8**, 2808 (1996); **9**, 2462(E) (1996).
[5] M. M. Fyrillas and A. J. Szeri, J. Fluid Mech. **277**, 381 (1994).
[6] D. Lohse, M. P. Brenner, T. F. Dupont, S. Hilgenfeldt, and B. Johnston, Phys. Rev. Lett. **78**, 1359 (1997).
[7] R. G. Holt and D. F. Gaitan, Phys. Rev. Lett. **77**, 3791 (1996); D. F. Gaitan and R. G. Holt, Phys. Rev. E **59**, 5495 (1999).
[8] U. H. Augsdörfer, A. K. Evans, and D. P. Oxley, Phys. Rev. E **61**, 5278 (2000).
[9] V. A. Bogoyavlenskiy, Phys. Rev. E **62**, 2158 (2000).
[10] L. Yuan, C. Y. Ho, M. C. Chu, and P. T. Leung, Phys. Rev. E **64**, 016317 (2001).
[11] R. Toegel, B. Gompf, R. Pecha, and D. Lohse, Phys. Rev. Lett. **85**, 3165 (2000).
[12] H. J. Liu and Y. An, Acta Phys. Sin. **52**, 620 (2003).
[13] M. P. Brenner, D. Lohse, and T. F. Dupont, Phys. Rev. Lett. **75**, 954 (1995).
[14] Y. Hao and A. Prosperetti, Phys. Fluids **11**, 1309 (1999).
[15] J. S. Dam, M. T. Levinsen, and M. Skogstad, Phys. Rev. Lett. **89**, 084303 (2002).
[16] M. T. Levinsen, N. Weppenaar, J. S. Dam, G. Simon, and M. Skogstad, Phys. Rev. E **68**, 035303 (R) (2003).
[17] J. A. Ketterling and R. E. Apfel, J. Acoust. Soc. Am. **107**, L13 (2000); Phys. Rev. E **61**, 3832 (2000).
[18] G. Simon, I. Csabai, A. Horvath, and F. Szalai, Phys. Rev. E **63**, 026301 (2001).